Reaction Dynamics of a Photochromic Fluorescing Dithienylethene

J. Ern,[†] A. T. Bens,[‡] H.-D. Martin,[‡] S. Mukamel,[§] S. Tretiak,[§] K. Tsyganenko,[⊥] K. Kuldova,[⊥,∥] H. P. Trommsdorff,[⊥] and C. Kryschi*[,†]

Lehrstuhl für Festkörperspektroskopie (IPkM), Heinrich-Heine-Universität, D-40225 Düsseldorf, Germany; Institut für Organische Chemie und Makromolekulare Chemie I, Heinrich-Heine-Universität, D-40225 Düsseldorf, Germany; Department of Chemistry, University of Rochester, Rochester, New York 14627; and Laboratoire de Spectrométrie Physique, Université Joseph-Fourier de Grenoble, CNRS (UMR 5588), B.P. 87, F-38402 St. Martin d'Hères Cedex, France

Received: September 6, 2000; In Final Form: November 8, 2000

The interplay of photochromism and fluorescence was studied by attaching anthracene as chromophore to dithienylperfluorocyclopentene (1,2-bis[5-anthryl-2-methylthien-3-yl]perfluorocyclopentene, Ac-BMTFP). The blue fluorescence of the open isomer of Ac-BMTFP is suppressed by the ring-closure reaction. The spectroscopic properties and the reaction dynamics of this compound were characterized by measurements of the fluorescence yield and decay dynamics, and the quantum yields of the photochromic ring-closure and ring-opening reactions, as well as the spectra and time evolution of reaction intermediates. The data are analyzed in terms of a model potential and single-electron density matrices, which are calculated using the collective electronic oscillator (CEO) approach and the INDO/S semiempirical Hamiltonian. For the ring-opening reaction, single-exponential decays with a time constant of 8 ± 0.5 ps were determined for the photoinduced bleaching and absorption transients. In contrast, because of the presence of reacting and nonreacting conformers, the dynamics measured for ring closure are more complex. Both conformers of the open isomer undergo a fast electronic−conformational relaxation on a time scale of ≈0.9 ps after excitation of the S_1 or S_3 state. Nonreacting conformers fluoresce with a distribution of lifetimes ranging from less than 100 ps to more than 400 ps. Reacting conformers reach a precursor state with a lifetime of 10 ps from which the ring-closure reaction takes place. The rates of the ring-opening and ring-closure reactions are determined as 9.5×10^9 and 6×10^{10} s^{-1}, respectively. Rather than being a drawback, the presence of different conformers in the sample is argued to be a requirement for applications relying on efficient switching of the fluorescence.

1. Introduction

Photochromic 1,2-bis[2-methylthien-3-yl]perfluorocyclopentene derivatives receive increasing attention as materials for the design of multi-stable switching units with light controlled electrochemical and optical properties.[1] These compounds combine a number of favorable properties: high stability and fatigue resistance, large absorption coefficients of the lowest energy transition, and large changes of the absorption wavelength between the two isomers. The photochromic electrocyclic reaction of this class of compounds (see Figure 1) obeys to the Woodward−Hoffmann rules applied to the π molecular orbital symmetries of cyclohexadiene (closed isomer) and hexatriene (open isomer).[2] Ring-opening and ring-closure reactions occur photochemically in the conrotatory mode, while the thermally induced ground-state ring-opening reaction, predicted to take place in the disrotatory mode, is sterically hindered by the two trans-oriented methyl groups at the 2-position of the thiophene rings. Upon UV irradiation, the open isomer undergoes a ring-closure reaction, while the ring-opening reaction is induced by excitation with visible light. Derivatives containing various chromophores have been designed and synthesized mainly with the goal to adjust the absorption maxima and to arrive at a better understanding of the reaction.[3] In addition, the introduction of a fluorescent chromophore in the 5-position of the thiophene rings was shown to lead to photoswitchable fluorescence properties.[4] Since only the open isomer fluoresces with significant yield, fluorescence is suppressed by the ring-closure reaction and is restored by the ring-opening reaction.

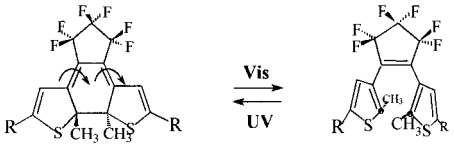

Figure 1. Structure formula of the closed (left) and open (right) isomer of Ac-BMTFP (R = anthryl; for the open isomer the a−p conformer is shown).

Previous time-resolved studies on the picosecond and femtosecond time scale of electrocyclic reactions in dithienylethene derivatives have shown that both ring-opening and ring-closure reactions occur on a time scale of 10^{-12} s.[5−9] In addition, slower

* Corresponding author. Present address: Institut für Theoretische und Physikalische Chemie I, Friedrich-Alexander-Universität Erlangen Nürnberg, Egerlandstr. 3, D-91058 Erlangen, Germany. Tel: 49-9131-8527307. Fax: 49-9131-8528796. E-mail: kryschi@pctc.chemie.uni-erlangen.de.

[†] Lehrstuhl für Festkörperspektroskopie (IPkM), Heinrich-Heine-Universität.

[‡] Institut für Organische Chemie und Makromolekulare Chemie I, Heinrich-Heine-Universität.

[§] University of Rochester.

[⊥] Université Joseph-Fourier de Grenoble.

[∥] On leave from Institute of Physics, AV CR Cukrovarnická 10, 16253 Prague, Czech Republic.

10.1021/jp0031956 CCC: $20.00
Published on Web 00/00/0000 PAGE EST: 8.5

SCHEME 1

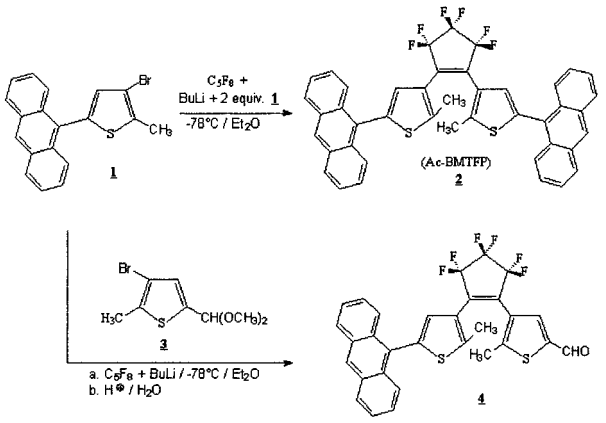

components have been identified.[5] Prior to the present work, the reaction kinetics of only five diethienylethene derivatives have been investigated.[5−9] Transient absorption studies of the maleic anhydride derivative in solution and of 1,2-bis[2,5-dimethylthien-3-yl]perfluorocyclopentene in solution as well as in the crystalline phase indicated that the time constants of the ring-opening and ring-closure reaction are shorter than 10 ps.[5,7] Analogous investigations of the open isomer of the oligothiophene derivative of BMTFP, with femtosecond time resolution, yield a ring-closure reaction time constant of about 1.1 ps.[6] The dynamics of the ring-opening reaction of 1,2-bis[2-methyl-5-(2-(4-benzoylphenylvinyl))thien-3-yl]perfluorocyclopentene in solution were investigated with femtosecond transient absorption spectroscopy and biexponential decays of the photoinduced absorption with the time constants of 1.9 and 9 ps were observed.[8] Very recently, we have reported studies of the ring-opening reaction of 1,2-bis[5-formyl-2-methylthien-3-yl]-perfluorocyclopentene (CHO-BMTFP) in dichloromethane solution.[9] The transients of photoinduced absorption and bleaching were analyzed in terms of a model potential based on calculations of the S_0, S_1, and S_2 potential energy hyperlines.[9] These calculations were performed within the collective electronic oscillator (CEO) approach developed by Mukamel and colleagues.[10] Within the first picosecond after excitation to the S_1 state, the closed isomer CHO-BMTFP undergoes a fast structural relaxation along the S_1 potential energy surface into the a precursor state of the ring-opening reaction. This precursor, with a fairly long lifetime of 13 ps, predominantly relaxes radiationless to the S_0 state of the closed isomer, while the rate constant of the ring-opening reaction is small, $k_{RO} \approx 3.1 \times 10^9\ s^{-1}$.

In the present study, we investigate the ring-closure and ring-opening reaction as well as the fluorescence decay dynamics of the anthryl-substituted BMTFP derivative (1,2-bis[5-Ac-2-methylthien-3-yl]perfluorocyclopentene, Ac-BMTFP; compound **2** in Scheme 1) in solution with time-resolved absorption and fluorescence spectroscopy.[11] In addition, to generate molecules with photoswitchable fluorescence properties, the introduction of a fluorescent chromophore offers opportunities to study the excitation energy flow and the reaction dynamics in chromophore-substituted BMTFP molecules. Indeed, the properties of these molecules are characterized by the competition between reactivity and fluorescence, governed by excitation-energy transfer and radiationless decay processes. The coupling of the electronic states of the chromophore and those of the central photochromic unit can in principle be controlled via the chemical and geometrical linkage between the two units. In the present case, a single bond links the two anthracene chromophores with the dithienylethene unit. The absorption spectra (see Figure 2)

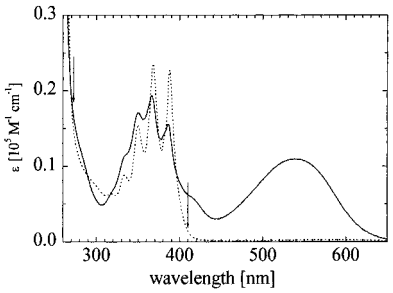

Figure 2. Absorption spectra of the open (dashed line) and closed (solid line) isomer of Ac-BMTFP in methylcyclohexane. The spectrum of the closed isomer was obtained by subtracting the spectrum of the open isomer from the measured spectrum of a mixture of both isomers. The arrows indicate the two excitation wavelengths used to induce the ring-closure reaction.

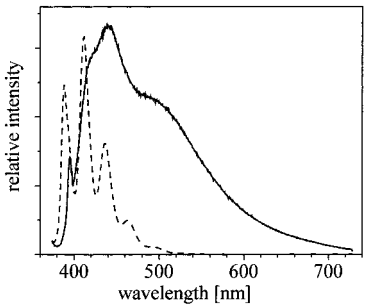

Figure 3. Fluorescence spectra of 9-methylanthracene (dashed line) and Ac-BMTFP (solid line) in cyclohexane. The line at 400 nm is a Raman line of the solvent.

demonstrate clearly that the lowest energy states can be well understood in terms of slightly perturbed states of the constituents for both the open and the closed isomers. The absorption is dominated by the strong contribution characteristic of anthracene, with little spectral shifts and some line broadening in the case of the closed isomer. It is interesting to note that the line broadening, resulting from the ring-closure reaction, is more pronounced in Ac-BMTFP than in the monoanthryl-substituted compound **2** (see Scheme 1). This effect illustrates the coupling of the two anthryl substituents across the closed isomer, absent in the open isomer. In contrast, the effect of coupling of the anthryl substituent to the central BMTFP unit is much more pronounced in fluorescence. Compared to methyl substituted anthracene, the fluorescence of the open isomer of Ac-BMTFP is not the mirror image of the lowest energy absorption but is significantly red shifted (see Figure 3) with a concomitant loss of vibrational structure and a reduction of the quantum yield to about 1%. Even though the S_1 excitation energy of the open isomer of Ac-BMTFP is significantly lower than that of unsubstituted BMTFP, the ring-closure reaction yield remains fairly high (10−30%) as does the yield of the ring-opening reaction (3−8%). The molecule is therefore well suited for a characterization of the reaction and excitation dynamics by transient absorption spectroscopy and time-resolved fluorescence studies. In addition, the excited states involved in these processes were characterized within a theoretical study based on the collective oscillator approach.[10]

The paper is organized as follows: in the following section 2, experimental details are given, with the details of the synthesis given in the Appendix. A theoretical description of the relevant excited states of Ac-BMTFP and of the reaction path is presented in section 3, and in section 4 the experimental results are given and discussed in terms of excited state and reaction dynamics. Finally, in section 5 we conclude.

2. Experimental Section

2.1. Transient Absorption Spectroscopy. Transient absorption spectra with femtosecond time resolution were measured using the pump−probe technique. Pump and probe pulses were generated by a femtosecond laser system, described previously,[9] which delivers pulses of 120 fs (260 fs in the UV) duration at a repetition rate of 600 Hz. For the pump beam the required UV wavelengths were obtained by frequency doubling and a white light continuum between 300 and 1000 nm was generated for the probe beam. The pump pulses passed through a variable delay line and were polarized at the magic angle relative to the polarization of the probe pulse. The excitation density was kept below 0.5 mJ/cm^2. The intensity of the transmitted probe beam with and without pump pulse excitation, $I(p)$ and $I(0)$, respectively, was measured by chopping the pump pulse beam at a frequency of 6 Hz. For each data point, 13 000 pulses were averaged.

The ratio $I(p)/I(0)$, which equals the pump pulse induced change of the transmittance, $\Delta T = T(p)/T(0)$, was determined with an accuracy of better than 10^{-2}. For the small changes recorded here, $1 - \Delta T$ equals the sum of the difference spectra of all species contributing to the signal, weighted by their respective concentrations:

$$1 - \Delta^T \propto \sum_i c_i(\epsilon_i(\lambda) - \epsilon_0(\lambda)) \qquad (1)$$

$\epsilon_i(\lambda)$ is the extinction coefficient of species i ($i = 0$ is the ground state) present in the sample with a relative concentration of c_i ($\sum c_i = 1$).

The time dispersion of 1.4 ps over the spectral range of the white-light continuum probe pulses was corrected for by determining at spectral intervals of about 80 cm^{-1} the $\tau_D = 0$ fs point from the rise of the bleaching or absorption transients. Transmission spectra of the sample were obtained by dispersing the probe pulses with a polychromator containing a 400 lines/mm grating in combination with a CCD detector system.

Ac-BMTFP was dissolved in spectrograde *n*-hexane (for the ring-opening reaction) or dichloromethane (for the ring-closure reaction, some measurements were also made in THF with virtually identical results) at a concentration of 6.4×10^{-4} mol/L. The solution was pumped at 5 mL/s through a 400 μm flow cell to ensure a complete renewal of the sample between pulses.

2.2. UV/Vis Absorption Spectroscopy and Chemical Actinometry. Commercially (Aldrich) available solvents were used. Absorption spectra were recorded with a Perkin-Elmer Lambda 9 spectrometer. Quantum yields were determined from the evolution of the absorption spectra after irradiation of the solutions for various intervals of time. The experimental error is ca. 10%. The intensities of the light sources were calibrated with furylfulgide actinometer aberchrome 540. The open isomers were irradiated with the UV lines of Ar$^+$ laser (351−363.5 nm), the closed isomers with the 514 nm Ar$^+$ laser line and/or with a 632 nm He−Ne laser. The concentrations of solutions for quantum yield measurements were at least 6×10^{-4} M in order to ensure total absorption of incident light.

2.3. Fluorescence Spectroscopy. Static fluorescence spectra were recorded and fluorescence quantum yields were determined by exciting a fresh sample with a single shot of the third or forth harmonic (355 nm, 266 nm) of a Nd:YAG laser and using a spectrometer (Chromex #500SH) with a grating of 150 grooves/mm, equipped with a cooled optical multichannel analyzer (OMA, Princeton Instruments ST130 LN/CCD). This procedure avoided any contribution of degradation products that were observed after prolonged irradiation. A 9-methylanthracene solution, for which the fluorescence quantum yield is known (0.32 in cyclohexane),[12] was used for calibration. The Raman line at 400 nm (see Figure 3) provided additional calibration of the spectra.

Some preliminary time-resolved fluorescence measurements were made with a Hamamatsu High-Performance Universal Streak Camera C5680. Fluorescence lifetimes were determined from time correlated single photon counting measurements. The excitation pulse was the second harmonic from a mode-locked Ti:sapphire laser Tsunami (Spectra-Physics Lasers) ($\lambda_{exc} \sim 380$ nm) pumped by an Ar$^+$ laser (Coherent). The detection system consisted of a Jobin Yvon monochromator, a microchannel plate photomultiplier (Hamamatsu R3809U-51), a constant fraction discriminator (Ortec 9302), a time-to-amplitude converter (Ortec 567), and an analog-digital converter (Wilkinson 12 bit). The instrument response was about 25 ps. The concentrations of the solutions in these measurements were below 10^{-4} M, in a range where results are concentration independent. Because of the evolution of the sample under laser irradiation and the limited supply of sample preventing the use of a flow system, a compromise had to be made between accumulation time and statistical noise of the decay curves in order to obtain reliable data. These factors influence less the transient absorption measurements, where difference spectra are recorded.

2.4. Syntheses. *General*. All syntheses, carried out under argon or nitrogen atmosphere, were monitored by TLC using aluminum-backed silica gel (230−400 mesh) or by HPLC using a Hewlett-Packard ChemStation 1040 and 1050 Series II instrument and were protected strictly from light. Octafluorocyclopentene was obtained as a donation from Bayer AG. Solvents and other reagents were used as purchased without further purification, unless stated otherwise. Column chromatography was performed on silica gel (230−400 mesh) using nitrogen or argon flushed solvents. Melting points: uncorrected, Reichardt Thermovar; NMR: Varian VXR 300 and Bruker DRX 500 at frequencies of 300 and 500 MHz for ^{1}H and 470 MHz for ^{19}F, respectively. Reference compounds were TMS (^{1}H) and $CFCl_3$ (^{19}F). UV/visible: Perkin-Elmer Lambda 19 spectrophotometer. IR: Perkin-Elmer 1420 spectrometer. EI-MS: Varian MAT 311A and MAT 8000.

The details of the synthesis are described in the Appendix.

3. Electronic-Coherence Signatures of Electrocyclic Reaction

The calculations, presented here, are analogous to the ones published previously for another diethienylethene derivative[9] and are summarized below.

3.1. Ground-State Electronic Structure and Geometry. The open isomer of Ac-BMTFP is predicted to exist in two different conformations: the so-called antiparallel (a−p) and parallel (p) conformations are obtained from the closed isomer by dis- and con-rotatory rotations of the thiophene rings and have local symmetry of C_2 and C_s, respectively (see Figure 1). The a−p conformation undergoes the ring-closure reaction, while the conrotatory rotation of the thiophene rings methyl groups is sterically hindered in the p conformation. The room-temperature population of both conformers was determined by calculating the heat of formation, ΔH_f, using the semiempirical AM1 model implemented in Gaussian 94,[13] as $\Delta H_f(p) = -5.6 \times 10^{-21}$ J and $\Delta H_f(a-p) = -9.3 \times 10^{-21}$ J. The population ratio, ρ_p/ρ_{a-p}, of the two conformers is given the Boltzmann distribution: $\rho_p/\rho_{a-p} = \exp(-\Delta E/kT)$ with $-\Delta E = -(\Delta H_f(p) - \Delta H_f(a-p))$ and equals $\rho_p \approx 19\%$ and $\rho_{a-p} \approx 81\%$. The following computations are made for the antiparallel open isomer only.

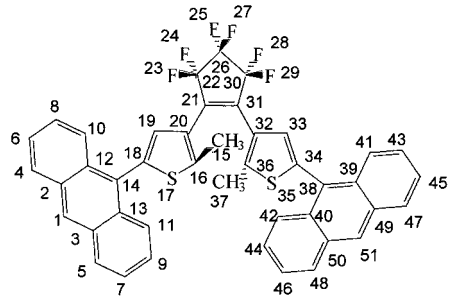

Figure 4. Structure formula of the closed isomer of Ac-BMTFP with the numbering of the "heavy" atoms: C, S, F, O.

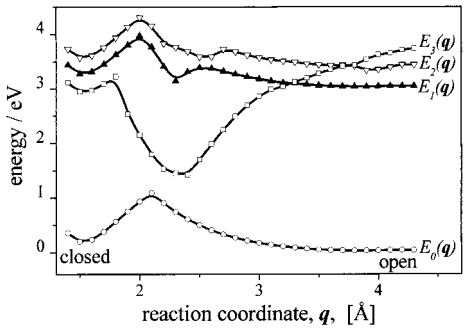

Figure 5. Potential energy hyperlines, $E_0(q)$, $E_1(q)$, $E_2(q)$, $E_3(q)$, along the reaction coordinate q (see text). The perturbation of the S_2 and S_3 states, visible in the region of $q = 2.2-2.7$ Å, is due to mixing with the S_4 state.

The ring-opening and ring-closure reactions of Ac-BMTFP were analyzed in terms of a model reaction potential composed of cuts along the reaction coordinate q of the potential energy surfaces of the S_0, S_1, S_2, and S_3 states. q is defined by the distance between the carbon atoms, **C16** and **C36** (*see* Figure 4), where the bond making and breaking take place, while the values of all other coordinates are those of the ground-state geometry, optimized at the AM1 level for this value of q. The associated ground-state energies, E_0, were determined using single configuration interaction (CI) computations within the semiempirical AM1 model and Gaussian 94 package.[13] q was varied between 4.3 and 1.4 Å in steps of 0.1 Å. The resulting S_0 potential energy hyperline, $E_0(q)$, is shown in Figure 5 (open circles). The optimized geometries of the closed and open isomers are localized at $q = 1.5$ Å and $q = 4.0$ Å and are separated by a large, 1 eV, potential barrier along the S_0 hyperline.

The geometry-optimized structural data were used as input data for the ZINDO code[14] to compute the INDO/S Hamiltonian parameters and reduced single-electron density matrices for the S_0 state, $\bar{\rho}_{mn}$:

$$\bar{\rho}_{mn} \equiv \langle 0|c_m^+ c_n|0\rangle \tag{2}$$

where $c_m^+(c_m)$ are creation (annihilation) operators of an electron at the mth atomic orbital, and $|0>$ is the ground state. The diagonal elements $\bar{\rho}_{nn}$ represent the electronic charge density at the nth orbital, whereas the off-diagonal elements $\bar{\rho}_{mn}$, with $m \neq n$, describe the bond-order (electronic coherence) structure associated with a pair of localized atomic orbitals. The ground-state density matrix $\bar{\rho}_{mn}$ is expanded in the basis set of the $2p_x$ atomic orbitals, which form the π-electron system. The differences in the π-electron conjugation are clearly reflected in the off-diagonal elements $\bar{\rho}_{mn}$: the π-electron system of the closed isomer is delocalized along the π-conjugated backbone (**C14**−**C18**−**C19**−**C20**−**C21**−**C31**−**C32**−**C33**−**C34**−**C38**) over the dithienylethene unit, while for the open isomer the π-conjugation is less extended.

3.2. Electronic Excitations along the Reaction Coordinate. The CEO technique[10] was then used to compute and analyze the optical spectra using $\bar{\rho}$ as input. The optical transitions between the ground state, $|0\rangle$, and excited states, $|\nu\rangle$, are described in terms of the transition density matrix elements:

$$(\xi_\nu)_{mn} = \langle \nu|c_m^+ c_n|0\rangle \tag{3}$$

The linear optical response is given by the frequency-dependent linear polarizability $\alpha(\omega)$:

$$\alpha(\omega) = \sum_\nu \sum_{mnkl} \mu_{mn}\mu_{kl} \frac{2\Omega_\nu(\xi_\nu)_{mn}(\xi_\nu)_{kl}}{\Omega_\nu^{\,2} - (\omega + i\Gamma_\nu)^2} \tag{4}$$

Here Γ_ν is the dephasing rate, and ν is the index of the excited singlet states, $|\nu\rangle$, with energies, E_ν, and transition frequencies, $\Omega_\nu = E_\nu - E_0$. The matrices ξ_ν and frequencies Ω_ν are determined by solving the time-dependent Hatree-Fock (TDHF) equations for the density matrix:

$$\rho_{mn}(t) \equiv \langle \psi(t)|c_m^+ c_n|\psi(t)\rangle = \rho_{mn} + \sum_\nu a_\nu(t)(\xi_\nu)_{mn} + a_\nu^*(t)(\xi_\nu^+)_{mn} \tag{5}$$

where $\psi(t)$ represents the wave function of the molecule driven by the external electromagnetic field. The equations were solved using the density matrix spectral moment algorithm (DSMA),[10] yielding ξ_ν and Ω_ν as eigenfunctions and eigenvalues of the linearized TDHF equation, respectively. The adiabatic potential energy surfaces of the excited states, S_1, S_2, and S_3, along the (ground state) reaction coordinate q are computed by adding at the each nuclear configuration, q, the energy of the electronic mode, $\Omega_\nu(q)$ with $\nu = 1, 2, 3$, to the energy of the ground state, S_0:[15]

$$E_\nu(q) = E_0(q) + \Omega_\nu(q) \tag{6}$$

The potential energy hyperlines, $E_1(q)$, $E_2(q)$, and $E_3(q)$, are shown in Figure 5. The electronic modes were obtained in the adiabatic approximation, and the hyperlines are not, by construction, minimum-energy paths on the excited-state potential energy surfaces. In addition, the solvent is not included in the calculation. Nevertheless, the resulting S_0 and S_1 hyperlines illustrate qualitatively the photochemical reaction funnel[16] in the region around $q \approx 2.1$ Å.

To study the variations of electronic density induced by photoexcitations, we further analyzed the transition density matrices ξ_ν. The diagonal elements, $(\xi_\nu)_{nn}$, represent the photoinduced net charge on the nth atomic orbital, and the dynamical bond order (or coherence) between the nth and mth atomic orbitals is given by the off-diagonal elements, $(\xi_\nu)_{nm}$ ($n \neq m$). The νth oscillator describes the optical transition between the ground state and the excited state, S_ν. In the case of ξ_1 (closed isomer), the delocalization of the S_0-S_1 optical excitation (exciton coherence) reaches its largest density along the **S17**−**C18**−**C19**−**C20**−**C21**−**C31**−**C32**−**C33**−**C34**−**S35** chain, while the excitation density at the anthryl substituents is about half of that at the dithienylethene unit. In contrast, ξ_3 (closed isomer) and ξ'_1 (open isomer) indicate a nearly complete localization of the S_0-S_3 or S_0-S_1 excitation on the anthryl substituents. The density matrix ξ'_3 (open isomer) represents

TABLE 1: Quantum Yields of the Ring-Opening and Ring-Closure Reactions Measured for the Ac-BMTFP in Different Solvents

	Ac-BMTFP (**2**)			**4**		
solvent	closure	opening	fluorescence	closure	opening	fluorescence
n-hexane	0.14	0.077				
cyclohexane	0.15	0.048	0.016	0.42	0.077	0.033
methylcyclohexane	0.22	0.070	0.012	0.36	0.069	0.009
toluene	0.21	0.032				
THF	0.32	0.064	0.005	0.29	0.060	0.003
acetonitrile	0.14	0.074	0.003	0.05	0.063	0.002
DMSO	0.08	0.058	0.004	0.04	0.049	0.004

an intermediate between localization of the optical excitation on the anthryl groups and on the photochromic unit. These differences in the calculated electronic modes are consistent with the observed change of electronic and optical properties during the ring-opening and ring-closure reaction. In particular, the observation of photoswitchable fluorescence agrees with the localization of the lowest energy optical excitation on the anthryl substituents of the fluorescing open isomer, while for the nonfluorescent closed isomer the maximum excitation density is located at the dithienylethene unit.

4. Experimental Results

4.1. Reaction Quantum Yields. The quantum yields of the ring-opening and ring-closure reactions measured for the Ac-BMTFP in different solvents are given in Table 1. For comparison, results obtained for the monoanthryl-substituted compound **4** (see Scheme 1) are also indicated. While the dependence of the ring-closure photoreaction for Ac-BMTFP on the solvent polarity follows no obvious trend and is not well understood, the quantum yield decreases with increasing solvent polarity in compound **4** (from 0.42 in cyclohexane to 0.04 in DMSO). The ring-opening quantum yields of both compounds are hardly affected by solvent polarity. Irie and Sayo have made similar observations for 1,2-bis(2,4,5-trimethylthiophene-3-yl)-maleic anhydride where the ring-closure reaction yield decreases from 0.13 in *n*-hexane to 0.0003 in acetonitrile, while the ring-opening yields change only from 0.16 to 0.10.[17]

4.2. Fluorescence: Spectra, Decay Dynamics, and Quantum Yield. (All measurements refer to the open isomer of Ac-BMTFP.) The fluorescence quantum yields of Ac-BMTFP and of compound **4** in different solvents are given in Table 1. The fluorescence quantum yield decreases with increasing solvent polarity (an effect also observed for the above-mentioned compound studied by Irie and Sayo.[17]

The static fluorescence spectrum of Ac-BMTFP (which is very similar to that of compound **4**) is shown in Figure 3 together with that of methylanthracene. In contrast to the S_0-S_1 absorption spectra of the two compounds, the fluorescence spectra differ significantly, a large red shift indicating a relaxation of the S_1 state of Ac-BMTFP. Note that this relaxation does not involve a substantial solvent reorganization, since the fluorescence spectra do not depend significantly on the nature (polarity) of the solvent. This relaxation of S_1 indicates a mixing of the locally excited anthryl state with the excited states of the central switch, but apparently does not involve a significant degree of net charge transfer, as observed in bianthryl and related compounds,[18] where the fluorescence is strongly solvent dependent. The mixing of states as a function of the reaction coordinate, q, is also apparent in the calculations presented in section 3. The electronic modes at intermediate distances indicate, for the open isomer of Ac-BMTFP, the onset of this mixing at distances not much shorter than the ground-state equilibrium value of q.

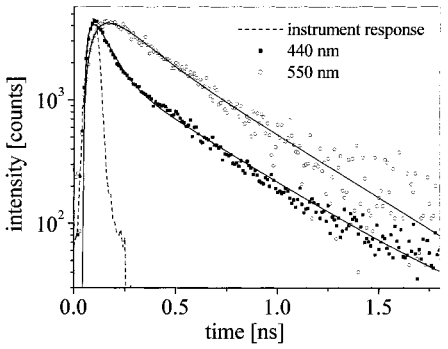

Figure 6. Fluorescence decay of Ac-BMTFP in dichloromethane, monitored at 440 and 550 nm, together with a fit of the data.

These static measurements can be used to derive information about the relaxation of the S_1 state of Ac-BMTFP, based on the following arguments: (i) the S_0-S_1 absorption spectra of methylanthracene and of Ac-BMTFP are virtually identical, except for a small broadening for the latter, (ii) the fluorescence of methylanthracene is the mirror image of the absorption, (iii) unrelaxed fluorescence of Ac-BMTFP should therefore also be the mirror image of the absorption spectrum. An evaluation of the contribution of unrelaxed fluorescence of Ac-BMTFP to the observed spectrum, shown in Figure 3, which is dominated by the relaxed fluorescence, was made and gives an upper limit of 1/25. The quantum yield of this unrelaxed emission is thus smaller than 5×10^{-4}, and the lifetime of the unrelaxed S_1 state of Ac-BMTFP is therefore ≤ 10 ps.

Streak camera measurements clearly indicate that the fluorescence spectra are not homogeneous. This observation was quantified by fluorescence decay measurements at different wavelengths. Figure 6 shows fluorescence decay curves of the Ac-BMTFP in dichloromethane detected at 440 and 550 nm after excitation at 380 nm. At 440 nm, the rise of the signal is limited by the instrument response (20−30 ps), while at 550 nm the rise is clearly slower: A rise with a time constant of about 70 ps is obtained in a single-exponential fit. The fluorescence decay is significantly faster than in 9-methylanthracene, for which a lifetime of 6.8 ± 0.2 ns (in dichloromethane) was obtained. The decay of the spectrum of Ac-BMTFP is not homogeneous but becomes slower in going to lower energies. Even though the decay is multiexponential, at any given wavelength, a biexponential fit is sufficient within the accuracy of the decay data. For the two decay curves shown in Figure 6, we obtain the following results: at 440 nm 75 ± 5 and 430 ± 30 ps with relative intensities in the ratio of 4.5/1; and at 550 nm 140 ± 10 and 430 ± 30 ps with relative intensities in the ratio of 1.5/1.

4.3. Transient Absorption Spectra. *Ring-Opening Reaction.* Figure 7 shows the time evolution of the transient spectra of the closed isomer of Ac-BMTFP in *n*-hexane. The spectra represent the transmittance changes, $\Delta T(\lambda,\tau_D)$, at different time intervals, τ_D, from −0.3 ps up to 34 ps after excitation at 512

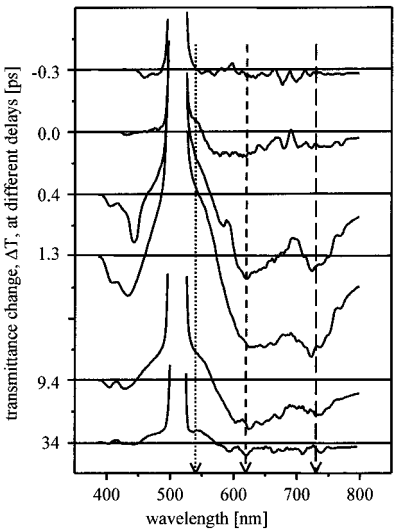

Figure 7. Temporal evolution of the transient absorption spectra of the closed isomer of Ac-BMTFP in *n*-hexane recorded at delay times τ_D between −0.3 and +34 ps. The excitation wavelength is 512 nm. The arrows indicate the wavelengths at which time profiles of the decay are given in Figure 10.

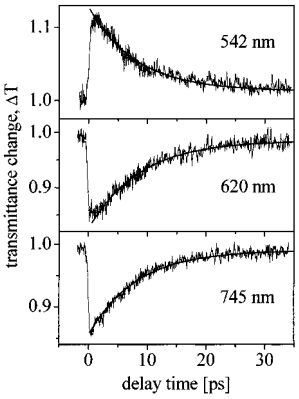

Figure 8. Transients of photoinduced changes at 542 nm (top), 620 nm (center), and at 745 nm (bottom). The pump-pulse wavelength is 512 nm.

nm. This excitation wavelength is tuned to the high-energy side of the S_0-S_1 absorption band. Both S_1-S_n absorption ($\Delta T < 1$) and ground-state bleaching ($\Delta T > 1$) contribute to the observed signals. The spectra at $\tau_D \leq -0.3$ ps provide the baseline with $\Delta T(\lambda) = 1$. Scattered pump-pulse light is responsible for the peak around 512 nm. Between 470 and ca. 570 nm the ground-state bleaching dominates, while the photoinduced S_1-S_n absorption is preponderant at longer wavelengths from 570 to 760 nm.

Examples of the time dependence of the photoinduced transmission changes at three fixed wavelengths, λ_{det} (i.e., $\Delta T(\tau_D,\lambda_{det})$), are shown in Figure 8. At $\lambda_{det} = 542$ nm, photoinduced bleaching is observed and transient absorption at $\lambda_{det} = 620$ and 745 nm. All signals decay, within experimental accuracy, homogeneously and monoexponentially with the same time constant of 8 ± 0.5 ps, which can therefore be safely attributed to the lifetime of the excited S_1 state of the closed isomer. Combined with the quantum yield of the ring-opening reaction (7.7%), given above (section 4.1), this measurement yields a rate constant for this reaction of $k_{RO} = 9.6 \times 10^9\ s^{-1}$.

Ring-Closure Reaction. In contrast to the simple kinetics observed for the ring-opening reaction, the dynamics of the ring-closure reaction is complex, because of the competition of the reactivity of the open isomer with fluorescence of the anthryl

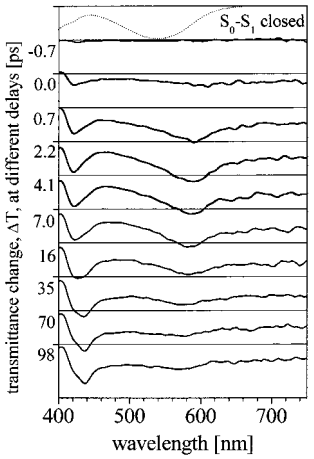

Figure 9. Temporal evolution of the transient absorption spectra of the open isomer of Ac-BMTFP in dichloromethane recorded at delay times τ_D between −0.7 and +98 ps. The S_0-S_3 transition of the open isomer is excited at 272 nm. The top panel shows the stationary absorption spectrum of the closed isomer.

substituents on the one hand, and the presence of different conformers on the other. Pump wavelengths of 410 and 272 nm have been used to initially excite more or less the anthryl substituents and the central photochromic unit of the open isomer of Ac-BMTFP (see Figure 2). In fact, the transient absorption spectra exhibit essentially the same features for the two pump wavelengths. Figure 9 shows transient spectra, recorded in dichloromethane and uncontaminated by scattered pump-pulse light at 272 nm exciting the S_0-S_3 transition, at delay times between −0.7 and +98 ps. The spectra at $\tau_D \leq -0.7$ ps provide the baseline with $\Delta T(\lambda) = 1$. The stationary absorption spectrum of the closed isomer (top panel of Figure 9) is given for comparison and shows the S_0-S_1 absorption band between around 540 nm and the onset of the S_0-S_2 transition around 420 nm. Transient absorption ($\Delta T(\lambda) < 1$) has two obvious contributions: one is the instantaneous S_1-S_n absorption of the open isomer, present at the earliest times, and the other is the stationary absorption spectrum of the closed isomer which should dominate at the longest times. In the spectral range shown, no ground-state bleaching signals contribute to the spectra.

In spite of the fairly simple appearance of the spectra in Figure 9, the temporal evolution of the different spectral components is complex. Clearly some of the spectral components are coupled, and decay times of one component equal the rise time of another, but the overall behavior can only be rationalized if the sample is assumed to be inhomogeneous. An analysis of the transient spectra was made through decomposition in spectral components. These components were forced to be identical in all spectra, only the amplitudes vary with time. In order to reduce the number of free parameters, components with near equal time evolutions were linked and forced to obey simple exponential growth and decay behavior in subsequent fits. This reduction of free parameters was achieved without significant loss of the quality of the fit. Figure 10 illustrates this decomposition for some of the transient spectra, the spectral components being marked a1 to a6.

Within the instrument response time, a broad (fwhm 4500 cm^{-1}) short-lived transient absorption band centered on 490 nm (a4) is observed. In order to evaluate the decay time of this signal, an analysis of time profiles was made via FFT, as shown in Figure 11. This analysis leads to a time constant of 0.9 ps for the transient species, which is attributed to the absorption of unrelaxed, initially excited state.

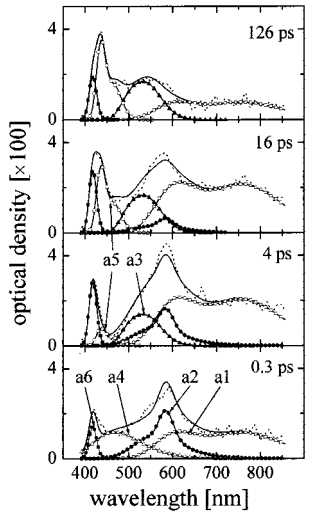

Figure 10. Example of the decomposition of some transient spectra (as shown in Figure 11) recorded at delays of 0.3, 4.0, 16, and 126 ps. The same spectral components, labeled a1 to a6, with different amplitudes are used in all fits.

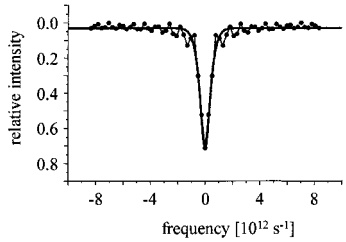

Figure 11. Fast Fourier transformation (FFT) into the frequency domain of the fast decay component of the transient spectra recorded for the ring-closure reaction of Ac-BMTFP (excited at 272 nm). Thin lines with solid circles: FFT of the data; thick solid line: fit of the data using the product of a Gaussian and a Lorentzian (see text).

Within the same time scale, longer-lived species are generated with absorption peaks at 420 nm (a6) and 585 nm (shoulder at 560 nm) (a2) as well as a broad structure at low energy at wavelengths longer than ca. 610 nm (a1). The 585/560) nm (a2) absorption decays on a time scale of 13 ps while the 420 nm peak (a6) has a lifetime of about 240 ps. The broad low-energy absorption (a1) decays on a ca. 120 ps time scale. Note that because of the limited time scale of the measurements the longer time constants are fairly imprecise (±40%). In parallel, a broad absorption background is observed which grows in time. The relative importance of this background at early times is the main difference between the 410 and 272 nm excitation. With time constants, which equal within experimental accuracy the decay of the 585/560 nm feature (a2), the growth of absorption bands at 435 nm (a5, rise time 14 ps) and 540 nm (a3, rise time 10 ps) is observed. The decay of these features is beyond the time scale of the experiment. While the short time constants determined from the fluorescence data are in agreement with the time constants observed here, the species giving rise to the slowest fluorescence decay may also contribute to the near stationary background. The evolution at long times due to nonreacting molecules in the p conformation which fluoresce and possibly other species generated by the excitation (triplet states and longer lived transient chemical species) is not of central interest here and will not be discussed in detail below.

A picture that emerges and that is consistent with the ensemble of observations and the calculations presented in section 3 is the following. In the solution coexist two conformers (a−p and p) of the open isomer and an additional subdistribution of conformations given by the rotation of the anthryl substituent around the single **C14−C18** (or **C34−C38**) bond. The calculated ratio of a−p to p conformers is 5:1, but this value is indicative only, being based on an energy difference of the conformers in vacuo. An experimental value can be determined by assuming that the radiative rate of Ac-BMTFP is approximately the same for the unrelaxed and relaxed state. The fluorescence quantum yield (1.2−1.6%) and lifetime (average 130−150 ps) measurements indicate that about 50% of the molecules are p conformers (this value decreases if the radiative rate of the relaxed state is lower). As first approximation we may thus assume that about 50% of the molecules are a−p conformers. The two conformers are kinetically isolated on the time scales of the measurements discussed here. Calculations, neglecting solvation, indicate a barrier of 330 meV between the two conformers. This barrier is essentially due to steric hindrance between the methyl groups and should therefore not change too much in solution. Given an attempt frequency of less than 10^{11} s^{-1}, the interconversion of the conformers is expected to take place on a microsecond time scale or longer.

Because of the similarity of the absorption spectra, the two conformers are about equally excited. Within 1 ps the initially excited state of either conformer undergoes an electronic−structural relaxation, since both short- and long-lived species are generated within this time scale. This relaxation is likely to take place along the reaction coordinate as discussed in section 4.2. For the p conformer, the conformational change is limited by the steric hindrance between the methyl groups and long-lived (≥100 ps) states are reached. The a−p conformer reaches a precursor state with a lifetime of 10 ps and from which the ring-closure reaction takes place and which is located on the hyperline $E_1(q)$ at distances of about $q \approx 3.2-3.5$ Å (Figure 5). It is likely that the broad transient feature a4 reflects the spectral narrowing of the absorption of the initially excited states of the distribution of conformers. The assignment of a3 to the closed isomer is obvious, while absorption features a1/a6 with lifetimes of 180 ± 60 ps are attributed to the relaxed fluorescent state of the p conformer. Although for anthracene these excited-state absorption bands have been identified at higher energies,[18,19] the assignment is plausible for the relaxed S_1 of Ac-BMTFP state since the energy differences are comparable to the shift from unrelaxed to relaxed fluorescence. The band a2 is naturally assigned to the precursor state, while band a5 may be due to the anthryl triplet state. From the data discussed above (50% a−p conformer, measured quantum yield of the ring-closure reaction ≈30% in THF, 10 ps lifetime of the precursor state), the rate of the ring-closure reaction is obtained as $k_{RC} = 6 \times 10^{10}$ s^{-1} and is thus about 6 times higher than the rate of the ring-opening reaction.

5. Conclusions

The present work represents a fairly complete characterization of the spectroscopic properties and the reaction dynamics of a fluorescent photochromic molecule, 1,2-bis[5-anthryl-2-methylthien-3-yl]perfluorocyclopentene. The coexistence of different conformers for this molecule is a complication in the analysis of the experimental results, but is also, in our view, a necessity when efficient photochromic and fluorescence properties are to be combined in a single molecule. Indeed, in order to achieve a high efficiency of photochromic reactions, the reaction rates must be high as compared to competing decay processes of the excited states, not only radiative but also other nonradiative processes. This requirement implies that fluorescence is also efficiently suppressed when the reaction rate is much higher

than the radiative decay rate. The presence of different conformers is a possibility to circumvent this dilemma, provided that the reactivity is inhibited in one of the conformers and the interconversion between conformers occurs on an appropriate time scale. This time scale must be short as compared to the irradiation time used to change the color of the sample, but should be long as compared to the lifetime of the excited state. Obviously, the coexistence of reacting nonfluorescent and fluorescent nonreacting conformers decreases the efficiency of both processes. However, this decrease is only by a factor of 2 for an approximately equal population of conformers. In the present case, the partial relaxation along the reaction coordinate of the nonreacting conformer is a likely cause of nonradiative decay, which decreases the fluorescence quantum yield from a theoretical value of 16% to about 1.6%. By proper design it should be easily possible to eliminate this deficiency. Nevertheless, efficient switching of fluorescence will not take place between on and off states but will generally be limited to switching between stronger and weaker fluorescence of a sample.

Acknowledgment. This research has been supported by the Volkswagenstiftung (Photonik, Az.: I/71 939) and by the National Science Foundation (Grants No. CHE-9526125). We are indebted to J-C. Vial for his help and the use of the fluorescence decay measurement setup.

Appendix

5-(9-Anthryl)-3-brom-2-methylthiophene (1). 60 g (234 mmol) of 3,5-dibromo-2-methylthiophene was dissolved in 400 mL of diethyl ether and was cooled to −78 °C. Within 45 min 146 mL (234 mmol) of 1.6 M *n*-butyllithium was added under an argon atmosphere to the intensive stirred yellow-colored solution. After an additional 30 min of stirring, a solution of 45.3 g (225 mmol) of anthrone in 800 mL of toluene was added dropwise within 60 min, resulting in an intensive orange-green fluorescent colored solution, which was stirred for an additional 1.5 h at −78 °C. The solution was allowed to warm slowly to room temperature, and the darkened solution was stirred for additional 2 h before it was poured onto a mixture of ice and water and was extracted with 500 mL of diethyl ether. The organic layer was washed several times with water. Evaporation of the organic solvent gave a orange-brown colored oil, which was thereafter dissolved in a mixture of 250 mL of ethanol and 250 mL of toluene. 100 mL of hydrochloric acid was added and the mixture was refluxed for 3 h. The cooled crude product was poured onto a mixture of ice and water. Extracted with 200 mL of diethyl ether, the solution was washed neutral with a diluted solution of sodium hydrogen sulfate and water. The organic layers were dried over $MgSO_4$ and chromatographed through silica gel (230−460 mesh) using a 3:1 dichloromethane/*n*-hexane mixture as eluent. Additionally, the yellow product was recrystallized in a 1:1 mixture of ethanol and toluene. The product was isolated and dried in vacuo at 0.1 mbar, yielding 56.84 g (mp 173−175 °C; 68.8% yield) of a yellow-colored solid:^{1}H NMR (500 MHz, $CDCl_3$): $\delta = 2.58$ (s, 3 H, $-CH_3$), 7.03 (s, 1H, H-4), 7.45−7.52 (m, 4H, H-2′ H-3′ H-6′ H-7′), 7.95 (d, 2H, H-4′ H-5′, $^3J_{3'-4'} = {}^3J_{5'-6'} = 8.8$ Hz), 8.06 (d, 2H, H-1′ H-8′, $^3J_{1'-2'} = {}^3J_{7'-8'} = 8.8$ Hz), 8.55 (s, 1H, H-10′). UV/vis (*n*-hexane) λ_{max} (log ϵ) = 258 (4.77), 351 (3.48), 369 (3.68), 390 (3.66). IR (KBr): $\tilde{\nu} = 733$, 855, 1442 ($-CH_3$), 1624, 1541, 1508 (aryl −C═C-), 3055 (aryl-H). MS (70 eV): *m*/*z* (%) = 352, 354 (92, 100) [$M^+ -1$], 272 (17) [$M^+ -$Br], 240 (25), 177 (8) [anthryl $C_{14}H_9+$], 136 (26), 129 (18), 56 (55) [C_4H_8+], 43 (60) [C_3H_7+], 32 (67) [S^+]. $C_{19}H_{13}BrS$ (353.27): calcd. C 64.40, H 3.71; found C 64.49, H 3.59

1,2-Bis-(5-(9-Anthryl)-2-methylthien-3-yl)perfluorocyclopentene (2). 11.29 g (32 mmol) of 5-(9-anthryl)-3-brom-2-methylthiophene (**1**) was dissolved under an argon atmosphere in 150 mL of freshly distilled diethyl ether ($LiAlH_4$) and was cooled to −78 °C with an acetone/dry ice bath. 21 mL (34 mmol) of 1.6 M *n*-butyllithium was added over 30 min. The mixture was stirred for additional 2 h at −78 °C before 3.18 g (32 mmol) of cooled octafluorocyclopentene was added through a rubber septum using a cooled syringe. Stirring at −78 °C was continued for 120 min. The cooling bath was then removed and the solution was allowed to warm to room temperature, continuing stirring for further 2 h. 500 mL of HCl (1%, v/v) was added to the now darkened brown-colored solution. The organic phase was washed several times with saturated sodium hydrogen sulfate solution and water. The water phases were also extracted with diethyl ether. The combined organic phases were dried over $MgSO_4$ and were evaporated, yielding a brown-colored crude solid. This crude product was chromatographed through silica gel (230−460 mesh) using a 4:1 mixture of *n*-hexane and dichloromethane as eluent, yielding 9.64 g (83.6%; mp 130−135 °C) of **2** as a light yellow-colored solid: ^{1}H NMR (500 MHz, $CDCl_3$): $\delta = 2.47$ (s, 6 H, $-CH_3$), 7.18 (s, 2H, H-4′), 8.06 (d, 4H, H-1″ H-8″, $^3J_{1''-2''} = {}^3J_{7''-8''} = 8.5$ Hz), 7.83 (d, 4H, H-4″ H-5″, $^3J_{3''-4''} = {}^3J_{5''-6''} = 8.5$ Hz), 7.31−7.34 (m, 4H, H-3″ H-6″), 7.46−7.49 (m, 4H, H-2″ H-7″), 8.57 (s, 2H, H-10″). ^{13}C NMR (500 MHz, $CDCl_3$): $\delta = 14.64$ ($-CH_3$), 125.31 (C-2″C-7″), 125.40, 125.98 (C-4″C-5″), 126.27 (C-3″C-6″), 127.12, 128.38 (C-1″C-8″), 128.41 (C-10″), 129.55 (C-4′), 131.12, 131.62, 137.31, 142.74. ^{19}F NMR (470 MHz, $CFCl_3$): $\delta = -126.20$ (s, 2F, F-4), −104.19 (s, 4F, F-3,4). UV/vis (*n*-hexane): (open form) λ_{max} (log ϵ) = 256 (5.04), 349 (3.83), 367 (4.01), 387 (3.99); (closed form) λ_{max} (log ϵ) = 533 (4.05).-IR (KBr): $\tilde{\nu} = 1268$ (C−F), 1442 ($-CH_3$), 1624, 1520 (aryl −C═C-), 3052 (aryl-H). MS (70 eV): *m*/*z* (%) = 721 (47) [M^+], 720 (100) [$M^+ -1$], 360 (22) [$M^+(2e^-)$], 177 (4) [anthryl $C_{14}H_9^+$], 56 (52) [$C_4H_8^+$], 43 (40) [$C_3H_7^+$], 32 (32) [S^+]. $C_{43}H_{26}F_6S_2$ (720.78): calculated. C 71.65, H 3.64; found C 71.68, H 3.93

1-(5-Formyl-2-methylthien-3-yl)-2-(5-(9-anthryl)-2-methylthien-3-yl)perfluorocyclopentene (4). 10.04 g (40 mmol) of 3-bromo-2-methyl-5-thiophenecarbaldehyde−dimethylacetal and 14.13 g (40 mmol) 5-(9-anthryl)-3-brom-2-methylthiophene (***1***) were dissolved under argon atmosphere in 250 mL of freshly distilled ($LiAlH_4$) diethyl ether and were cooled to −78 °C with an acetone/dry ice bath. 53.2 mL (85 mmol) of 1.6 M *n*-butyllithium was added, dropwise, over 30 min and then stirred for 1 h at −78 °C. 8.51 g (40 mmol) of cooled octafluorocyclopentene was added to the intensively stirred solution at −78 °C. Stirring at this temperature was continued for an additional 90 min before the cooling bath was removed and the orange solution was allowed to warm slowly to room temperature, continuing stirring for additional 3 h. 500 mL of HCl (1%, v/v) was added to the now darkened brown solution. The organic phase was washed several times with saturated sodium hydrogen sulfate solution and water. The water phases were also extracted with diethyl ether. The combined organic phases were dried over $MgSO_4$ and were evaporated, yielding 30.98 g of a yellow-brown-colored crude oily solid. This crude product contained the unsymmetrical product (**4**), the bis(anthryl) product (**2**), and the dimethylacetal protected bis(aldehyde). This solid was dissolved in 200 mL of methanol and 800 mL of diluted HCl (1% v/v) was added and the mixture was stirred

overnight at room temperature. The water phase was extracted with 1000 mL of diethyl ether and after removal of the solvents the crude product was chromatographed through silica gel (230−460 mesh) using a 2:1 mixture of *n*-hexane and dichloromethane as eluent, yielding 4.79 g (20.91%; mp 130−135 °C) of **4** as a light yellow-colored solid. Additional amounts of the bis(aldehyde) (ca. 25%) and the bis(anthryl) product **2** (ca. 35%) were obtained. Characterization of **4** gave ^{1}H NMR (500 MHz, $CDCl_3$): δ = 2.19, 2.34 (s, 6H, $-CH_3$), 7.08 (s, 2H, H-4′), 8.07 (d, 2H, H-1″ H-8″, $^3J_{1''-2''} = {}^3J_{7''-8''}$ = 8.1 Hz), 7.79 (d, 2H, H-4″ H-5″, $^3J_{3''-4''} = {}^3J_{5''-6''}$ = 8.0 Hz), 7.46−7.53 (m, 4H, H-3″ H-6″ H-2″ H-7″), 8.57 (s, 1H, H-10″), 9.90 (s, 1H, CHO). ^{13}C NMR (500 MHz, $CDCl_3$): δ = 14.59 and 15.54 ($-CH_3$), 124.64, 125.39, 125.73, 126.39, 126.72, 126.75, 128.55, 128.63, 129.13, 131.17, 131.56, 136.43, 137.93, 141.88, 143.20, 151.52, 182.08 (CHO). ^{19}F NMR (470 MHz, $CFCl_3$): δ = −126.11 (s, 2F, F-4), −104.34 (s, 4F, F-3 and F-5). UV/vis (*n*-hexane): (open form) λ_{max} (lg ϵ) = 255 (4.79), 332 (3.47), 349 (3.65), 367 (3.80), 386 (3.77); (closed form) λ_{max} (log ϵ) = 586 (4.05). IR (KBr): $\tilde{\nu}$ = 1269 (C−F), 1442 ($-CH_3$), 1455, 1541 (aryl −C═C−), 1671 (CHO), 3053 (aryl-H). MS (70 eV): *m*/*z* (%) = 572 (100) [M^+], 553 (12) [M^+ −F], 286 (12) [M^+ ($2e^-$)], 178 (42) [anthryl $C_{14}H_{10}^+$], 56 (47) [$C_4H_8^+$], 43 (49) [$C_3H_7^+$]. $C_{30}H_{18}OF_6S_2$ (572.58): calculated. C 62.93, H 3.17; found C 62.76, H 3.17.

References and Notes

(1) Irie, M. *Jpn. J. Appl. Phys.* **1989**, *28*, 215. Uchida, K.; Nakayama, Y.; Irie, M. *Bull. Chem. Soc. Jpn.* **1990**, *63*, 1311. Irie, M.; Uchida, K. *Bull. Chem. Soc. Jpn.* **1998**, *71*, 985. Gilat, S. L.; Kawai, S. H.; Lehn, J.-M. *J. Chem. Soc., Chem. Commun.* **1993**, 1439. Gilat, S. L.; Kawai, S. H.; Lehn, J.-M. *Chem. Eur. J.* **1995**, *1*, 275. Tsivgoulis, G. M.; Lehn, J.-M. *Angew. Chem.* **1995**, *107*, 1188; Irie, M. *Chem. Rev.* **2000**, *100*, 1685, and references therein.

(2) Woodward, R. B.; Hoffmann, R. *The Conservation of Orbital Symmetry*; Verlag Chemie: Weinheim, Germany, 1970.

(3) Bens, A. T.; Frewert, D.; Kodatis, K.; Kryschi, C.; Trommsdorff, H. P.; H.-D. Martin, *Eur. J. Org. Chem.* **1998**, 2333.

(4) Fernandez-Acebes, A.; Lehn, J.-M. *Adv. Mater.* **1998**, *10*, 1519. Takeshita, M.; Irie, M. *Chem. Lett.* **1998**, 1123. Kasatani, K.; Kambe, S.; Irie, M. *J. Photochem. Photobiol. A: Chem.* **1999**, *122*, 11.

(5) Miyasaka, H.; Araki, S.; Tabata, A.; Nobuto, T.; Mataga, N.; Irie, M. *Chem. Phys. Lett.* **1994**, *230*, 249.

(6) Tamai, N.; Saika, T.; Shimidzu, T.; Irie, M. *J. Phys. Chem.* **1996**, *100*, 4689.

(7) Miyasaka, H.; Nobuto, T.; Itaya, A.; Tamai, N.; Irie, M. *Chem. Phys. Lett.* **1997**, *269*, 281.

(8) Ern, J.; Bens, A. T.; Bock, A.; Martin, H.-D.; Kryschi, C. *J. Lumin.* **1998**, *76/77*, 90.

(9) Ern, J.; Bens, A. T.; Martin, H.-D.; Mukamel, S.; Schmid, D.; Tretiak, S.; Tsiper, E.; Kryschi, C. *Chem. Phys.* **1999**, *246*, 115.

(10) Tretiak, S.; Cherniak, V.; Mukamel, S. *J. Am. Chem. Soc.* **1997**, *119*, 11408. Mukamel, S.; Tretiak, S.; Wagersreiter, Th.; Chernyak, V. *Science* **1997**, *277*, 781. Chernyak, V.; Mukamel, S. *J. Chem. Phys.* **1996**, *104*, 444.

(11) Tsyganenko, K. Ph.D. Thesis, Université Joseph-Fourier Grenoble I, 1998. Ern, J. Ph.D. Thesis, Heinrich-Heine-Universität, Düsseldorf, 2000.

(12) Nijegorodov, N. I.; Downey, W. S. *Spectrochim. Acta* **1995,** *A51*, 2335.

(13) Fritsch, M. J., et al. *Gaussian-94*; Gaussian Inc.: Pittsburgh, PA, 1995.

(14) Zerner, M. C.; Loew, G. H.; Kirchner, R. F.; Mueller-Westhoff, U. T. *J. Am. Chem. Soc.* **1980**, *102*, 589.

(15) Tsiper, E. V.; Chernyak, V.; Tretiak, S.; Mukamel, S. *Chem. Phys. Lett.* **1999,** *302*, 77. Tsiper, E. V.; Chernyak, V.; Tretiak, S.; Mukamel, S. *J. Chem. Phys.* **1999**, *110*, 8328.

(16) Klessinger, M. *Pure Appl. Chem.* **1997**, *69*, 773. Celani, P.; Ottani, S.; Olivucci, M.; Bernardi F.; Robb, M. A. *J. Am. Chem. Soc.* **1994**, *116*, 10141. Michl J.; Bonacic-Koutecky, V. *Electronic Aspects of Organic Photochemistry*; Wiley: New York, 1990.

(17) Irie, M.; Sayo, K. *J. Phys. Chem.* **1992**, *96*, 7671.

(18) Jurczok, M.; Plaza, P.; Martin, M. M.; Meyer, Y. H.; Rettig, W. *Chem. Phys.* **2000**, *253*, 339.

(19) Bebelar, D. *Chem. Phys.* **1974**, *3*, 205.